



# The Impact of MISR-derived Injection Height Initialization on Wildfire and Volcanic Plume Dispersion in the HYSPLIT Model

Charles J. Vernon<sup>1</sup>, Ryan Bolt<sup>1</sup>, Timothy Canty<sup>1</sup>, Ralph A. Kahn<sup>2,1</sup>

<sup>1</sup>Atmospheric and Oceanic Science Department, University of Maryland, College Park, MD 20742,  
USA

<sup>2</sup>NASA Goddard Space Flight Center, 8800 Greenbelt Rd, Greenbelt, MD 20771, USA

**Abstract.** The dispersion of particles from wildfires, volcanic eruptions, dust storms, and other aerosol sources can affect air quality and other environmental factors downwind. Aerosol injection height is one source attribute that mediates downwind dispersion, as wind speed and direction can vary dramatically with elevation. Using plume heights derived from space-based, multi-angle imaging, we examine the impact of initializing plumes with satellite-measured vs. nominal (model-calculated or VAAC observations) injection height on the simulated dispersion of six large aerosol plumes. When there are significant differences in nominal vs. satellite-derived particle injection heights, or if one injection height is within the planetary boundary layer (PBL) and the other is above the PBL, differences in simulation results can arise. In the cases studied with significant nominal vs. satellite-derived injection height differences, the NOAA Air Resources Laboratory's Hybrid Single-Particle Lagrangian Integrated Trajectory (HYSPLIT) model tends to represent plume evolution better if the injection height in the model is constrained by hyper-stereo satellite retrievals.



## 1. Introduction

More than 5.5 million people worldwide die prematurely every year due to household and outdoor air pollution (Forouzanfar et al., 2015). Model forecasting of airborne particle dispersion is the essential tool used to alert citizens to possible poor air quality conditions, as well as to assess longer-term exposure. Aerosol plume height is a key input to these models (Walter et al., 2016). The height of aerosol plumes produced by wildfires, volcanic eruptions, and dust storms has a large impact on where the particles are transported, and their environmental impacts. If the aerosols are injected into the atmosphere above the planetary boundary layer (PBL) – or if they are entrained into the free troposphere after injection – they can be transported vast distances by free-tropospheric winds, causing aviation hazards, impacting regional-scale temperatures, cloud properties, and precipitation, and ultimately affecting ground-level air quality at great distances from the source (e.g., Colarco et al., 2004). To measure these plume heights near-source with reasonable certainty, we use hyper-stereo imagery from the NASA Earth Observing System’s Multi-angle Imaging SpectroRadiometer (MISR) instrument.

### 1.1. Multi-angle Imaging SpectroRadiometer (MISR) and MODerate resolution Imaging Spectroradiometer (MODIS)

The MISR instrument flies aboard the Terra satellite, in the AM constellation of the NASA Earth Observing System (EOS). Terra is in a near-polar orbit at an altitude of 705 km, descending on the dayside, with an equator crossing of 10:30 am local time, and completes an orbit in about 99 min. Each circuit of the Earth falls into one of 233 overlapping “paths” that repeat precisely every



16 days (Diner et al., 1998). The instrument acquires imagery at nine angles ranging from 0° (nadir) to 70° off-nadir in the forward and aft directions along-track, in each of four spectral bands centered at 446 (blue), 558 (green), 672 (red), and 866 nm (near infrared, NIR). Data are acquired routinely at 275-m horizontal resolution in the nadir view and in the red band of the other eight cameras; all other channels are obtained at 1.1 km resolution. The MISR design allows it to image every scene at nine viewing zenith angles along the satellite ground track, in seven minutes. The width of the MISR swath common to all cameras is about 380 km, providing global coverage every nine days at the equator and every two days near the poles. The MISR plume-height products are derived from the hyper-stereo imagery geometrically, and take account of the proper motion of plume elements. This retrieval approach requires contrast features in the plume to be visible in the multi-angle data. As such, MISR plume-height mapping complements aerosol height curtains obtained from space-based lidar; lidar offers sensitivity to thin aerosol layers downwind of sources, where plume features required for stereo image matching are lacking, but the active sensor offers vastly less spatial coverage, so the actual source regions are seldom observed (Kahn et al., 2008).

We also use context imagery from the two MODerate resolution Imaging Spectroradiometer (MODIS) instruments; one flies aboard the Terra satellite with MISR, and the other is aboard NASA's Aqua satellite. MODIS is a wide-swath, multi-spectral, single-view imager that acquires data over the entire planet every day or two, depending on latitude. MODIS can track the development of aerosol plumes over several days, allowing us to compare plume evolution, as simulated by different model runs, with imagery and aerosol optical depth (AOD) retrievals from MODIS.



## 1.2. The MISR Interactive eXplorer (MINX)

To apply the multi-angle capabilities of MISR most effectively for mapping aerosol plume height, the MISR Interactive eXplorer (MINX) interactive visualization application was developed (Nelson et al., 2013), complementing the fully automatic but less accurate operational MISR stereo product. MINX offers users a tool to retrieve height and wind information interactively at high spatial resolution and enhanced precision. Users operating the MINX interface must manually identify the horizontal extent of the plume in the imagery, the source point, and the wind direction; some user discretion is involved, and especially if significant wind runs along-track, small differences in the choice of wind direction can affect the resulting height retrieval (Nelson et al., 2013). Vertical resolution is between about 275 and 500 m, depending on observing conditions. This makes it possible to study the 3D context of a scene, and allows the user to detect scene content that would otherwise be difficult to discern in single-view imagery from more conventional satellite instruments such as MODIS. MINX retrievals were performed using MISR red band observations for this study, as it provides the highest spatial resolution at all MISR view angles, as well as the blue band imagery, which offers better contrast with the surface when the plume is optically thin.

## 1.3. The HYSPLIT Model

The National Oceanic and Atmospheric Administration (NOAA) Air Resources Laboratory's (ARL) Hybrid Single-Particle Lagrangian Integrated Trajectory model (HYSPLIT) is a complete system for computing simple air parcel trajectories as well as complex transport, dispersion, chemical transformation, and deposition simulations. HYSPLIT continues to be one of



the most extensively used atmospheric transport and dispersion models in the atmospheric sciences community (Stein et al., 2016). Some examples of previous work with HYSPLIT include tracking and forecasting the release of radioactive material, wildfire smoke, wind-blown dust, pollutants from various stationary and mobile emission sources, allergens, and volcanic ash (e.g., Stunder et al., 2007; Kahn and Limbacher, 2012; Crawford et al., 2016). The model calculation method can be Lagrangian, using a moving frame of reference for advection and diffusion calculations as the air parcels move from their initial location, Eulerian, which uses a fixed three-dimensional grid as a frame of reference to compute pollutant air concentrations, or a hybrid combination of the two approaches (Stein et al., 2016).

As with any such model, several factors can limit the accuracy of simulations, including uncertainty in the input pollutant injection height (Stein et al., 2009). Since the late 1990's, "The IAVW (International Airways Volcano Watch) has recognized that more accurate source parameters are needed to improve model accuracy, especially in the first hours of an eruption when few observations may be available" (Mastin et al., 2009). Although MISR data are acquired over a given location on Earth only about once per week on average, when available, these observations can improve forecasted plume dispersion. In this paper we explore the impact of using the unique data provided from MISR-MINX to obtain direct-source initial conditions to input into HYSPLIT. With the help of accurate plume heights, we can run the HYSPLIT dispersion model and compare the results with those obtained using the model's nominal injection height and with the actual dispersion of the plume as observed by MODIS.



## 2. Methods

We chose specific wildfire and volcanic eruption cases where the MINX retrievals are available and of high quality. MINX retrievals are not always available for specific events if MISR does not have coverage, or if there is significant cloud contamination of the scene. The quality of a case is determined by a lack of cloud contamination and sufficient optical thickness so contrast features in the aerosol plume are clearly visible in the imagery and distinct from the surface. The optical thickness criterion is assessed through visual inspection of each scene using the MINX camera animation function. The cases selected for this study are (1) the Mount Etna eruption of July 2001, (2) the Chikurachki Volcano eruption of April 2003, (3) the Eyjafjallajokull eruption of May 2010, (4) the Fort McMurray fires of May 2016, (5) the Fraser Plateau fires of August 2017, and (6) the Thomas fires of December 2017.

### 2.1. MINX Data

The plume injection height, source elevation, and precise location for each event were extracted from MINX and used as initial conditions in HYSPLIT. Figure 1a shows an example of the MINX height retrievals from analysis performed on the Eyjafjallajokull case, and Figure 1b gives the corresponding MINX height profile for that scene. Figure 1c provides the distribution of height retrievals at different levels along with the wind speeds diagnosed in MINX. Note that the red and blue points in the profile plot show the heights assuming zero wind, and the wind-corrected heights, respectively. Wind-corrected data were used in all cases for the current study. The MISR overpass, and corresponding MINX injection height for each case, was acquired on Day 1 of the



respective simulations. The MISR run of the dispersion model was then continued with the Day 1 MISR aerosol injection height for a total of four days (96 hours).

## 2.2. HYSPLIT Setup

We explore the effects of using multi-angle imaging via MISR to initialize HYSPLIT  
5 through *qualitative* analysis of the trajectory, dispersion, and indirect correlation between total  
column AOD and plume column mass concentration. To compare *absolute* emission amounts, we  
would need to specify particle property details such as the mass extinction efficiencies, which are  
very uncertain, and are not required to address the main goals of the current study. In addition,  
10 introducing emissions estimates, e.g., from BlueSky or the field-reported volcanic eruption rates,  
would introduce yet more uncertainty to the comparisons. (BlueSky is a fire and smoke prediction  
tool that uses the fire burn-scar size and location to estimate fire characteristics  
(<https://www.arl.noaa.gov/hysplit/smoke-prescribed-burns/>). Instead, we compare the relative  
simulation results using the same emissions, which entails fewer assumptions.

Volcano and wildfire plumes are initialized differently in the nominal HYSPLIT operation.  
15 Wildfire injection height is calculated dynamically throughout the simulation from an estimated fire  
heat flux and local meteorological conditions, whereas volcano injection height is generally input  
based on external observations. Between four and six particle sizes can be assumed for each  
volcano case, based on reporting from the Volcanic Ash Advisory Center (VAAC) responsible for  
region in which the eruption occurred. Each particle size makes up a portion of the total plume  
20 mass as defined by the particle size distribution from the VAAC report. Volcanic ash particle size



distribution options are discussed in more detail in Leadbetter et al. (2011), and the values for the cases considered in the current paper are listed in Table 1. Wildfire cases have only one assumed particle size in the nominal HYPLSIT process.

The following sections elaborate upon the nominal and MINX initialization procedures.

### 5 2.2.1. Volcano Plume Simulations

In order to create the nominal and MISR-initialized simulations, we followed the procedure specified for the VAAC Operational Dispersion Model Configuration

([https://www.wmo.int/aemp/sites/default/files/VAAC\\_Modelling\\_OperationalModelConfiguration-March2016\\_v3.pdf](https://www.wmo.int/aemp/sites/default/files/VAAC_Modelling_OperationalModelConfiguration-March2016_v3.pdf)). Unlike the operational HYSPLIT set up, our “nominal” runs used MINX-

10 derived source locations and source elevations. Operationally, eruption information from the Smithsonian Global Volcanism program is used to determine source location and elevation. We chose instead to use the location and elevation from MINX, due to its high resolution and ability for the user to determine the exact location of the eruption. However, in practice there was little difference between the GVP-listed and MINX-derived source locations. Also unlike the

15 operational system, we used constant injection heights, determined by the MISR-estimated plume height at the specific time of the relevant overpass for the MINX cases, and constant plume height as derived from the VAAC advisory nearest in time to the overpass for the nominal volcano cases. In the operational setting, injection height estimates are generally updated with each new forecast (e.g., every 6 hours), and the operational simulations are designed to take advantage of these

20 updated heights. And for both the nominal and MINX simulations, each is set up as a line source





from the vent to the maximum height of the plume, so it is assumed to have uniform mass distribution from the source to the injection peak.

To better isolate the impact of injection height on downwind plume dispersion, the MINX runs were configured exactly the same as the nominal runs, except for this variable. All other  
5 aspects of the simulation are determined by the VAAC reports and are defined in the operational configuration document cited above, including horizontal concentration-output grid spacing, particle size distribution (PSD), particle density, number of particle types, deposition settings, maximum altitude of the model, etc. As the values for these parameters reported by different  
10 VAACs can vary, our simulations aimed to match the configuration of the VAAC region in which the eruption occurred. The only exception is Chikurachki, which was set up with the Washington/Anchorage rather than the Tokyo VAAC configuration, due to its proximity to the Washington/Anchorage VAAC border and the fact that Washington/Anchorage uses HYSPLIT for their operational simulations.

As these simulations are meant to recreate short-to-medium range air quality forecasts for  
15 recent eruptions, we initialize the plume heights for the nominal cases based on VAAC advisories, if available, or the Global Volcanism Program (GVP) otherwise. The VAAC observations are likely to be released first and be the best first estimates for operational simulations. VAAC advisories that occurred closest to the time of the MISR overpass were used. The VAAC plume-height estimates are derived from ground-based or aircraft-based visible observations, from radar measurements, or  
20 from thermal infrared satellite soundings. In addition to the observational techniques used, plume height estimation can be determined based on an empirical relationship between plume height and



mass eruption rate, in the rare case that there are no direct observations available. All these methods, especially visible observations, come with notable uncertainties. A comparison between volcanic plume height from pilot reports, MINX heights, and ground-based plume-height assessments for volcanoes on the Kamchatka peninsula concluded that pilot reports were subject to the greatest uncertainties (Flower and Kahn, 2017). Radar-return heights generally skew toward the highest particle-rich part of the plume, satellite-based infrared retrievals sometimes must be corrected for thermal disequilibrium effects, and visual observations tend to encounter difficulties tracking the highest parts of plumes that are ash-poor (Mastin et al., 2009).

For the MISR-initialized simulations, the injection heights are determined as the maximum heights obtained from the MINX histogram of plume contrast-element elevations at MISR overpass time. The MINX injection heights, nominal injection heights, and boundary layer heights obtained from near-coincident meteorological soundings, are given in Table 1. Unlike the VAAC injection-height observations, the uncertainty in the MINX digitizations can be quantified, and for the red-channel retrievals used in the current study, it is only around 250 m.

As all three volcanic eruptions covered in this study occurred outside North America, the use of global meteorological data was required. Therefore, we were limited by the resolution at which global forecast models were archived during the time period of these eruptions. The coarseness of the meteorological data introduces some additional uncertainty into these simulations.

The Global Data Assimilation System (GDAS) 1.0° meteorological fields were chosen for the Eyjafjallajökull eruption case, and Final (FNL) Operational Global Analysis 1.0° meteorological data was used for eruptions that occurred before 2007. The data sets can be found in



HYSPLIT-compatible formats on the NOAA Air Resources Laboratory (ARL) meteorological data archive website (<ftp.hysplit.noaa.gov>). The GDAS system is used by the National Center for Environmental Prediction (NCEP) Global Forecast System (GFS) model to place observations into a gridded model space for the purpose of starting, or initializing, weather forecasts with observed data (<https://www.ncdc.noaa.gov/data-access/model-data/model-datasets/global-data-assimilation-system-gdas>). The FNL product is made with the same model NCEP used in the GFS, but the FNLs are prepared about an hour after the GFS is initialized, so more observational data can be applied (NCEP, 2000).

In summary, we are evaluating only the impact that more certain MINX injection height observations have on HYSPLIT downwind plume dispersion, and not the processes within the model.

### 2.2.2. Wildfire Plume Simulations

For wildfires, the configurations are based on NOAA's Smoke Forecasting System (SFS) operational HYSPLIT simulations defined in Rolph et al. (2009). The meteorological data fields used when that document was written was hourly, 12 km horizontal resolution North American Mesoscale – Weather Research and Forecasting (NAM-WRF) fields. More recently, special high-resolution nested grids were added to the weather forecasting models in regions with active major fires to further increase the resolution. However, the present study focuses on large-scale plume dispersion over longer simulation periods, 96 hours vs. the operational 72 hours. As such, we used more skillful but lower-resolution GDAS 0.5° meteorological data. In a comparison of major



numerical weather prediction models, it was found that the NAM was consistently the least skillful in short range forecasts of mean sea level pressure, and was subject to more error on the US west coast, which is where all of our wildfire simulations take place (Wedam et al., 2009). Although higher resolution meteorological fields like the NAM12 are able to resolve smaller-scale features such as sea breezes and complex terrain, we found that the advantages of higher spatial resolution were compensated by lower model predictive skill, leaving the overall results of the study independent of the meteorological fields chosen. A comparison of simulations performed with both the GDAS 0.5° and NAM12 km fields can be found in the Thomas Fire analysis in Section 3.3 below.

As in standard HYSPLIT operational runs, smoke plume-rise is calculated within the model based on the atmospheric stability, wind speed (both from the meteorological data), friction velocity, and a model-input heat flux derived from an analysis of output data from the United States Forest Service BlueSky fire emissions model (<https://www.airfire.org/bluesky>). In addition to the heat flux, the BlueSky model is used to estimate the emission rate of particulate matter less than 2.5 µm in diameter (PM<sub>2.5</sub>). The injection height calculated nominally by the model is given in the HYSPLIT “MESSAGE” file, which provides a diagnostic output of plume rise emission height and co-located mixed layer height above ground level (AGL) at every hour of the simulation. In the nominal case, the injection height is *dynamically varied throughout the simulation* based on variation in heat release and atmospheric conditions, and the emissions at any time during the simulation are released at the model-estimated final plume rise at that time and location in the model.



The plume height of the MISR-initialized cases is determined through the MINX digitization and as with the volcano cases, is defined as a line source from the fire elevation to maximum plume height. In the MISR-initialized simulations, this maximum plume height is kept constant throughout the simulation, at the value determined at the specific time of the MISR  
5 overpass, which occurs on Day 1 of the simulation. As it is unrealistic for the injection height to remain at the same height for the entirety of the simulation, a vertical line source from the ground to this constant maximum height is used in the MISR-initialized case. This creates mass release in the MINX-initiated cases at levels between the surface and injection layer, accounting to some extent for lower-elevation injection with diurnal boundary layer expansion and contraction and other  
10 atmospheric profile changes. The particle properties assumed for both nominal and MINX simulations are the nominal HYSPLIT values: spherical particles with an average diameter of 0.8  $\mu\text{m}$  and a density of  $2 \text{ g cm}^{-3}$ , identical to the operational product (Rolph et al., 2009). Where the operational configuration and ours differ is in the source locations, as they are defined by MISR instead of MODIS/GOES, and the duration of the simulations, which are extended from 72 to 96  
15 hours, to provide a more comprehensive view of the effects of a more accurate injection height. The fire simulations are typically set to output average concentrations in one layer from 0-5 km above ground level. Although smoke plumes rarely exceed the 5 km level, the cases in the present study include some extreme fires that regularly do. So an additional difference between our nominal simulations and the operational system is that ours are set to output average concentrations in one  
20 layer from 0-10 km above ground level.

### 2.2.3. General Configuration



In order to evaluate the atmospheric transport and dispersion predictions in the HYSPLIT simulations, we use the MODIS 3 km resolution level 2 AOD data set (MOD04\_3K and MYD04\_3K for Terra and Aqua MODIS, respectively; <https://ladsweb.modaps.eosdis.nasa.gov>) and accompanying MODIS visible imagery. To assess the ability of the model to simulate plume evolution, we output column mass concentration snapshots from HYSPLIT at the time of MODIS overpass for each day of the simulations, averaged from 0 to 10 km MSL to obtain a total column average concentration, and compare with the MODIS total column optical depth. To create comparable products, each run is performed from the beginning of the event until 96 hours later, outputting a plot coincident with every MODIS Terra overpass, or MODIS Aqua if a Terra overpass is unavailable. We plot each nominal and MISR-initialized HYSPLIT column mass concentration in arbitrary mass concentration units, as discussed in the next section.

### 2.3. Evaluation

To analyze the results of this study, we associate high-AOD regions from MODIS with areas where column mass integrated between 0 and 10 km elevation (i.e., the column mass concentration), is high, as determined by HYSPLIT. We test this assumption by comparing the spatial contours of HYSPLIT column mass concentration with the MODIS AOD maps (Supplemental Material Figure 1), by visual inspection. We then compare the conclusions drawn from the HYSPLIT concentration contour vs. MODIS AOD analysis with MODIS true color imagery, to identify any apparent spatial distribution differences and to associate smoke or volcanic aerosol opacity in the imagery with column concentration levels. The levels are represented by the



colored hexagons in Figures 2a and 2b, where the color represents concentration level and the hexagon represents a HYSPLIT output grid cell. The mass concentration in each output grid cell is summed and assigned to a bin corresponding to the concentration. The bin values indicate relative mass concentration, at intervals increasing by half an order of magnitude, based on the simulations.

5 The bin scale itself reports relative concentration values ranging from 0 (no mass) to 6 (most mass), in intervals of 1. For example, a value that falls within the “Very High” range is placed into bin 6. A value corresponding to the “Haze” range is placed into bin 3. The same mass concentration scale is used for all cases in this study. We adopted this approach to avoid over-interpreting the data – mass concentration differences within a bin are unlikely to be significant, whereas we have much

10 more confidence in the relative differences indicated by results falling into different bins. The HYSPLIT output grid cells are  $0.25^\circ$  latitude by  $0.25^\circ$  longitude for the wildfire cases and vary by VAAC for the volcanic cases as reported in the WMO documentation.

Figures 2a and b present a snapshot at hour ~42 of the 96-hour HYSPLIT simulations of for 0 – 10 km, vertically integrated, qualitative smoke plume concentrations for the Fort McMurray

15 wildfire, beginning 06 May 2016. All daily snapshot samplings of the model runs from each case are available in the supplemental material. The fuchsia and dark blue levels denote places where particles were present but where the AOD is expected to be too low for the smoke or ash to be visible in the MODIS imagery. The cyan level denotes smoke or ash that is either not visible or slightly visible (haze), but should still have moderate optical depth values. The green level indicates

20 where smoke should be easily visible from the satellite imagery and should have moderately high optical depth values. The orange level is where aerosol column concentrations are high and



corresponding optical depth values should be very high, with patches of missing data where the AOD is too high for MODIS to observe to the surface. The red level represents the highest column concentrations of aerosols in the simulation, and should have no optical depth data because the smoke or ash would be too thick for MODIS AOD retrievals.

5           The difference plot (Fig. 2c) uses the same scale for all cases and is based on the difference between the mass concentration bins assigned to each output grid cell by the nominal- vs. MISR- initialized simulations. The dark blue contour represents much higher column concentrations predicted in the nominal than the MISR-initialized simulation, and has a value of -4 or lower. The cyan contour represents slightly higher column concentrations forecasted for the nominal than the  
10 MISR-initialized simulation, and has a value of -2 or -3. The white contour represents column concentrations predicted to be very similar in both simulations, having values of -1, 0, or 1. The orange and red contours represent output grid cells where the column mass concentration is predicted to be slightly higher or significantly higher, respectively, in the MISR-initialized simulation than the nominal one. To be assigned to the orange bin, the difference has the value 2 or  
15 3. To be assigned to the red bin, the difference value must be 4 or higher. For example, a grid cell in the nominal simulation assigned to the “Very High” bin will have a value of 6. That same grid cell in the MISR-initialized simulation might be assigned to the “Visible” bin with a value of 4. Therefore the “MISR – Nominal Difference” value for that cell would be a -2 (“Nominal Slight”).

20           When assessing simulated atmospheric transport model performance, we compare the edges of the visible plumes in the satellite imagery with the qualitative green, cyan, or higher column mass concentration levels in the corresponding HYSPLIT images. In areas of cloud interference, as





observed in the visible imagery, it is not possible to verify whether the aerosol concentrations determined by the model correspond to observation, unless the smoke or ash is above the cloud layer. Also, this verification method utilizes total column mass concentration average and total column AOD, so it does not assess vertical plume structure, which is beyond the scope of the current work.

### 3. Results

One factor that determines the impact of the injection height on plume dispersion is whether the injection height is above the planetary boundary layer (PBL). As wind speed and direction are generally different within vs. above the PBL, a model simulation is much more likely to approximate observations if the assumed injection height is on the correct side of this boundary. Based on MISR stereo retrievals, Kahn et al. (2008) found that about 18% of wildfires in the boreal forest regions of Alaska and western Canada injected smoke above the PBL, and Val Martin et al. (2010), found that overall, approximately 4-12% of wildfire plumes in North America inject above the boundary layer into the free troposphere. Whether a plume is injected above the PBL depends primarily on the dynamical heat flux produced by the fire, the atmospheric stability structure, and the amount of entrainment of ambient air into the rising plume that occurs (Kahn et al., 2007). The time of day is a related factor, due to diurnal boundary layer expansion and contraction. The PBL tends to be well mixed, and usually grows deeper with solar heating during the day. The inversion at the top of the PBL helps confine smoke and other pollutants within its boundary; late in the day, as solar heating diminishes, the PBL typically collapses toward the surface. Winds within the



boundary layer tend to show distinct differences from the more predictable and often stronger winds aloft. In many cases, low-altitude wildfire injection heights were represented well in the nominal model, and resulted in very similar simulations to the MISR-initialized simulations. For the purposes of this study, we have chosen some cases that are very similar and some that show larger differences, to give a scope of the impact of injection height has on HYSPLIT. Snapshots taken of the model, on each of the four days of each simulation, are available in supplemental material.

We now compare in detail the performance of HYSPLIT downwind, for three fire and three volcanic plume cases initialized using MISR-MINX plume injection height and with the nominal model value.

### 3.1. Fort McMurray Fire Plume, May 2016

Of the four days for the Fort McMurray wildfire simulation, May 7<sup>th</sup>, 2016 (figure 2) best displays the differences between the nominal and MISR-initialized simulations. On the first simulated day of the event, MINX injection heights were higher than the PBL, based on both the atmospheric sounding from the nearby YSM airport and the GDAS meteorological fields included in Table 1. The nominal plume rise at the time of MISR overpass was also determined to be above the PBL based on the GDAS and the sounding as well. Of all of the wildfire cases studied, the nominal plume rise calculation for the Fort McMurray simulation also seemed to perform the best relative to the plume rise observed by MISR. However, as the simulation continues, the nominal injection height, which varies based on the HYSPLIT model, begins to diverge from the MINX value, which was acquired on Day 1, and differences appear in the simulations. The model injection



height, PBL height, and wind speeds for Day 2 of the Fort McMurray simulation are shown in Figure 3a for the sounding on May 8, 2016 (00 UTC ) at Fort Smith, just north of Fort McMurray. The boundary layer depth is discernable on the sounding by the inversion in temperature and rapid relative humidity decrease at about 2.5 km. The injection height as determined by MISR was 4.2 kilometers MSL and was set nominally by HYSPLIT at about 2.4 kilometers MSL at the time the MISR snapshot was acquired. Unlike the injection height calculated by HYSPLIT on Day 1 of the simulation, the nominal injection height for Day 2 is below the PBL. From the differences in wind speed and direction at each level it is clear that poor injection height initialization will affect the accuracy of downwind air quality forecasts. Figure 2 shows the MISR-initialized and nominal simulations, MISR-initialized minus nominal difference plots, and MODIS true color imagery for the Fort McMurray wildfires on Day 2 of the simulations. The MODIS AOD is shown in Supplemental Material, Figure 1a. Although the overall plume shapes, trajectories, and concentrations seem relatively similar, the difference plot reveals a significant deviation (Figure 2c). In the northwestern corner of the outlined portion of the plume, the MISR-initialized simulation displays higher aerosol concentrations than does the nominal one. When compared to the optical depth and visible imagery, the northern portion of this feature is covered in clouds, so the aerosol is obscured in the satellite data, but the southern portion is visible. The visible image has an optically thick, well-defined plume in the same area as the MISR-initialized case, favoring the MISR simulation, and the AOD map shows very high aerosol concentrations. There are missing data points in the AOD map, further indicating that concentrations are very high, as there is a lack of cloud cover in the visible imagery.



### 3.2. Fraser Plateau Fire Plume, August 2017

The Fraser Plateau case study (Figure 4) is an example of the impact that meteorology and a relatively uniform wind profile can have on dispersion simulations. Table 1 shows an approximate 0.6 km plume rise underestimation in the nominal case at the time of the MISR overpass. By Day 2 of the simulation, that difference had grown to approximately 1.4 km, although the actual injection height may have decreased as well. The sounding from ZXS Prince George on Day 2 of the simulation (Figure 3b) shows the PBL to be at approximately 3.1 km, the MINX injection height above the PBL, and nominal injection height below the PBL. In the case studies examined here, simulations in disagreement about injection height being above or below the PBL generally show significant differences. However, based on figure 3b, the winds above the PBL are also fairly consistent with those below the inversion in this case, generally coming from the north around 10-15 knots. In addition, about half of the plumes simulated in the MISR-initialized case are injected below the 3.1 km PBL. So even with some plumes that exceed the PBL, the wind shear differences are not significant enough to create large discrepancies, as we saw in the Fort McMurray case.

Differences in plume dispersion between the nominal HYSPLIT and MINX-initialized simulations shown in Figure 4c do not exceed “slight,” and there are very few such differences. Higher smoke concentrations coincide with visible smoke in the true color images, and MODIS AOD mapping is also consistent. This is true for hour 42.3 of the simulation, where visible smoke appears in the southeastern corner of the MODIS image. Even this far into the simulation and approximately 1000 km downwind, visible smoke can be seen entering the Montana region, in agreement with the



visible imagery, highlighting the accuracy of both the MISR-initialized and nominal simulations for this case.

### 3.3. Thomas Fire Plume, December 2017

The Thomas Fire was an ideal case for testing the differences between meteorological fields having different spatial resolutions. Theoretically, the NAM12 higher resolution meteorological data used in the current comparison would be more effective at resolving the fairly complex terrain and mesoscale meteorological processes such as sea breezes that might operate here. However, we know that the NAM lacks the skill the ECMWF and GFS models can achieve, even at coarser resolution. Figures 5 and 6 show Day 4 of the Thomas Fire simulation ran with GDAS 0.5° and NAM12 meteorological data, respectively. The overall plume dispersion is quite similar between the GDAS and NAM simulations. One of the most apparent differences between the GDAS and NAM simulations can be seen in the difference plots themselves (Figure 5c and 6c). The locations where the differences occur are almost identical, but the nominal vs. MINX differences are more prominent in the NAM12 plot. The areas where the nominal simulation is slightly higher, such as the eastern and southern edges of the visible plume, still exist in the NAM12 version but are much more prominent. The portion on the western edge of the visible plume where the MISR-initialized simulation was significantly higher also still exists, but with larger differences. So, even in a location with complex terrain and mesoscale meteorological processes affecting the simulations, the plume dispersion simulations are similar, and the overall results are independent of the meteorological data spatial resolution.



In contrast to the Fraser Plateau fire, there were significant differences in vertical wind speeds with elevation for the Thomas Fire. There was also a large difference in the nominal and MINX injection heights; on Day 1, 1.9 and 5.5 km mean sea level (MSL), respectively (Table 1). Although these values apply to the higher of the two plumes simulated, even the lower plume reached an elevation of 4.4 km MSL, indicating a difference of approximately 2.5 – 3.6 km between the nominal and MINX injection heights at MISR overpass time. Figure 5 shows the snapshots of each simulation on December 13 at 19:15 UTC, which is over 90 hours after the initialization of this simulation. Although both simulations perform well, especially considering how many hours after initialization this snapshot is taken, it is clear that the MISR-initialized simulation performed better, based on the difference plot in Figure 5c. Whereas the nominal simulation predicts slightly higher smoke concentrations near the southern edges of the outlined visible plume, it also predicts higher concentrations outside the visible plume that do not coincide with the contemporaneous visible imagery or AOD mapping. In addition, the MISR-initialized simulation predicts much higher smoke concentrations in the western portion of the visible plume outline, where the AOD is high and the visible imagery shows a dense band of smoke extending to the north/northeast.

The stronger advection that likely carried the smoke further in the westerly direction can be attributed to the stronger winds aloft shown in Figure 3c. At the MINX injection height, winds are out of the northeast at approximately 25 – 30 knots. The nominally calculated injection height is located around 1.9 km MSL, where the winds are light and variable around 5 knots.

### 3.4. Eyjafjallajökull Volcanic Eruption Plume, May 2010



For the volcanic cases, it is common for the injection heights of each plume to overshoot the height of the boundary layer due to the explosive nature of many such events. The nominal HYSPLIT injection heights are constrained by external data, so in many cases, the differences between the injection height obtained from the VAAC and the corresponding MINX value are not large. In addition, the meteorological conditions tend to be less variable with elevation within the free troposphere than between the free troposphere and the PBL, so detecting differences between the nominal and MISR-initialized HYSPLIT simulations can be more difficult than for wildfires. The VAAC advisory for the first day of this eruption reported plume heights at 6.7 km near MISR overpass time, whereas the MINX-derived injection height showed a maximum height of about 5.8 km. Although 0.9 km is a significant difference in injection height, Figure 3d shows winds at these two levels within 5 knots of each other, and are in nearly the same direction. This can account for the nearly identical dispersion snapshots in Figure 7.

By comparison with the visible imagery and AOD, both simulations reproduce the eruption well. The dispersion of the main plume extending from the vent is captured with high precision, and is constrained within the visible plume outline on each figure. Near-source concentrations are also both high, as seen in the true color image. Both simulations predicted a higher-concentration patch of ash on the eastern end of the laterally moving portion of the plume, which is apparent in the visible imagery (circled portion) as well. Although they both slightly misplace this portion of the plume, this snapshot was taken over 60 hours after initialization. The presence and general location of such a small feature helps to emphasize the accuracy of HYSPLIT when initialized with accurate injection heights.



### 3.5. Mount Etna Volcanic Eruption Plume, July 2001

The distinctions between the nominal and MISR-initialized cases for the Mount Etna eruption are also subtle compared to the wildfire cases discussed above. The observed PBL height is about 1 kilometer in the sounding of Figure 3e. The MINX injection height is at about 5.5 kilometers, and the nominal HYSPLIT injection height equals approximately 5.2 kilometers. As expected, with injection height initializations this close the plume dispersion is almost identical. Differences between the simulations would be difficult to identify without the assistance of the difference plot in Figure 8c. In this figure, concentration differences do not exceed the “slight” category, further showcasing the agreement. However, the MISR-initialized simulation does indicate the presence of slightly higher ash concentrations on the northeastern portion of the plume and the nominal indicates the slightly higher ash concentrations on the southwestern portion of the plume. Neither of these features can be verified due to the sun glint affecting these areas, but the near-source portions of the plume in both simulations have high correlations with the plume outlines the visible imagery.

### 3.6. Chikurachki Volcanic Eruption Plume, April 2003

The final case of the study was the Chikurachki eruption of April 2003 (Figure 8) on the Kamchatka Peninsula. The Figure 3f sounding and Figure 9 maps take place on the final day of the simulation, approximately 84 hours after HYSPLIT initialization. For this case, the MINX injection height is 4.2 kilometers and the nominal value is about 6.1 kilometers. As indicated in figure 3f, the PBL height near this overpass time was around 1.3 kilometers, so both injection heights are well above this layer. However, as in previous cases, there can still be significant differences depending





on vertical wind shear and meteorology. Figure 3f also shows that winds are about 30 knots faster at 6 kilometers than at 4 kilometers, and the wind direction is slightly more out of the west aloft as well. This suggests that near-source concentrations would not be as high in the nominal as the MINX-initialized simulation, because the plume particles would be advected away more quickly, and with a more easterly trajectory, for the nominal simulation. Both plots in figure 9 support these predictions, and in addition, the plume shape is more accurately modeled in the MISR-initialized simulation. When comparing each run with the visible imagery and visible plume outlines, the nominal case has a significantly wider visible plume than the MISR-initialized plume, which captures the visible portion almost exactly. Due to the discrepancy in the height initialization, the nominal case does not perform as well as the MISR-initialized one for near-source aerosol concentration, plume trajectory, and plume shape in the portion of the plume that can be verified in the cloud-free imagery.

#### 4. Conclusions

In this paper, we present a detailed analysis of the impact injection-height initialization has on the downwind plume simulations by the HYSPLIT model, for six well-defined wildfire smoke and volcanic aerosol plumes. In many cases, plume dispersion is accurately represented in both the nominal and MISR-initialized simulations. However, when injection is above the PBL, and especially if the nominal and MISR disagree about whether the plume is injected above the PBL, significant differences can appear in the simulated plume evolution. Even if both simulations are initialized above the PBL, as in most volcanic cases, the VAAC advisories used to initialize



HYSPLIT in the analysis shown here tend to overestimate the height, subjecting the simulated plume to different meteorological conditions. Based on this study, it appears that the availability of additional injection height constraints via MINX can help to improve simulated plume dispersion for wildfire and volcanic ash plumes using HYSPLIT.

5           It also seems that wildfire simulations can be more sensitive to variations in injection height than volcanic simulations. This is likely because wildfires frequently inject smoke near the PBL – free-troposphere boundary, where small changes in elevation can produce large changes in ambient wind speed and direction. However, volcanic simulations can also be improved where MINX injection heights are available. Model estimation of wildfire plume rise remains a challenging scientific problem (e.g., Val Martin et al., 2012). Yet, we note that MISR provides global coverage only about once per week on average, and the trade-off between initializing a simulation with more accurate MINX injection heights several days prior to a time of interest, vs. using less-accurate injection heights derived by a model closer to the time of interest, would depend on the particulars of the case involved. In future work, we hope to evaluate the wildfire plume-rise algorithms in  
10           HYSPLIT by comparison with plume rise estimates from MINX. If the evaluation shows that improvements can be made, we hope to develop new approaches to more accurately simulate plume rise.  
15

          As assessing plume rise specifically was not the main goal of this research, the use of half-degree meteorological data was deemed sufficient to assess the large-scale plume dispersion  
20           analyzed here. However, finer spatial resolution, non-hydrostatic meteorological fields will be important for evaluating plume rise on smaller scales, especially in the complex terrain



environments typical of many wildfires. As there are many variables in addition to plume injection height that affect the accuracy of HYSPLIT simulations, future work might include constraining model simulations with other information provided by satellite instruments. For example, MISR aerosol type (Kahn et al., 2001; Limbacher and Kahn, 2014) could be used to initialize HYSPLIT  
5 instead of the operational particle characteristics from the SFS and VAACs. In addition, other instruments, such as CALIPSO downwind aerosol layer heights and ground-based sensor AOD and particle properties, can help increase confidence in long-range smoke or volcanic aerosol dispersion forecasting.

Another next step would be to quantitatively evaluate the aerosol column mass  
10 concentration values and ground-level concentrations in HYSPLIT simulation results. More research into the relationship between the mass extinction coefficient and aerosol optical depth is needed to address this issue, as this quantity determines the relationship between column-integrated AOD and aerosol column mass concentration. If the values can be reliably converted, quantitative analysis becomes possible, expanding upon the qualitative results shown in this study. But even  
15 with the qualitative results presented here, we have demonstrated the influence aerosol injection height uncertainty can exert over simulation results, highlighting the importance of further efforts to reduce the uncertainty in these estimates for real-world emissions situations. We have also demonstrated that the use of MINX injection heights, when available, can improve downwind dispersion forecasts in the HYSPLIT model.

20



## Acknowledgements

We thank Mark Cohen and Alice Crawford from NOAA for providing assistance with the volcano simulations presented here. Mark also participated in reviewing early versions of the manuscript to assure accurate representation of the HYSPLIT model simulations. The work of C.J. Vernon and R. Bolt is supported in part by a grant from the NASA Earth Science Applications program, under L. Friedl. Vernon is also funded in part by T. Canty in part by a grant from the NASA Atmospheric Composition Program under R. Eckman. The work of R. Kahn is supported in part by the NASA Climate and Radiation Research and Analysis Program under H. Maring and the NASA Atmospheric Composition Modeling and Analysis Program under R. Eckman.

## References

- Colarco, P. R., Schoeberl, M. R., Doddridge, B. G., Marufu, L. T., Torres, O., and Welton, E. J. 2004. Transport of smoke from Canadian forest fires to the surface near Washington, D.C.: Injection height, entrainment, and optical properties. *J Geophys. Res.* 109, 2156-2202. doi: 10.1029/2003JD004248
- Crawford, A. M., B. J. B. Stunder, F. Ngan and M. J. Pavolonis (2016). "Initializing HYSPLIT with satellite observations of volcanic ash: A case study of the 2008 Kasatochi eruption." *Journal of Geophysical Research-Atmospheres* 121(18): 10786-10803.
- Diner, D. J., Beckert, J. C., Reilly, T. H., Bruegge, C. J., Conel, J. E., Kahn, R. A., Martonchik, J. V., Ackerman, T. P., Davies, R., Gerstl, S. A. W., Gordon, H. R., Muller, J.-P., Myneni, R. B., Sellers, P. J., Pinty, B., and Verstraete, M. M.: Multi-angle Imaging SpectroRadiometer (MISR) instrument description and experiment overview, *IEEE T. Geosci. Remote*, 36, 1072–1087, doi:10.1109/36.700992, 1998.
- Flower, V., and R.A. Kahn, 2017. Assessing the altitude and dispersion of volcanic plumes using MISR multi-angle imaging: Sixteen years of volcanic activity in the Kamchatka Peninsula, Russia. *J. Volcanology and Geothermal Research* 337, 1–15.
- Forouzanfar, M.H. et al. 2015. Global, regional, and national comparative risk assessment of 79 behavioural, environmental and occupational, and metabolic risks or clusters of risks in 188 countries, 1990–2013: a systematic analysis for the Global Burden of Disease Study 2013. *The Lancet.*, 386. doi: 10.1016/S0140-6736(15)00128-2



- Kahn, R.A., P. Banerjee, and D. McDonald, 2001. The Sensitivity of Multiangle Imaging to Natural Mixtures of Aerosols Over Ocean, *J. Geophys. Res.* 106, 18219-18238.
- 5 Kahn, R., Li, W., Moroney, C., Diner, D., Martonchik, J., & Fishbean, E. (2007, Jun 7). Aerosol source plume physical characteristics from space-based multiangle imaging. *J. Geophys. Res.*, 112. doi:10.1029/2006JD007647
- 10 Kahn, R., Chen, Y., Nelson, D., Leung, F., Li, Q., Diner, D., & Logan, J. (2008, Feb 22). Wild Smoke Injection Heights: Two Perspectives From Space. *Geophys. Res. Lett.*, 35. doi: 10.1029/2007GL032165
- 15 Kahn, R. & Limbacher, J. (2012, Oct 22). Eyjafjallajökull volcano plume particle-type characterization from space-based multi-angle imaging. *Atmos. Chem. Phys.*, 12. doi: 10.5194/acpd-12-17943-2012
- Leadbetter, S.J. & Hort, M.C. (2011). Volcanic ash hazard climatology for an eruption of Hekla Volcano, Iceland. *J. Volcanol. Geotherm. Res.*, 199. doi: 10.1016/j.jvolgeores.2010.11.016
- 20 Limbacher, J.A., and R.A. Kahn, 2014. MISR Research-Aerosol-Algorithm: Refinements For Dark Water Retrievals. *Atm. Meas. Tech.* 7, 1-19, doi:10.5194/amt-7-1-2014.
- 25 Mastin, L.G., Guffanti, M., Servranckx, R., Webley, P., Barsotti, S., Dean, K., Durant, A., Ewert, J.W., Neri, A., Rose, W.I., Schneider, D., Siebert, L., Stunder, B., Swanson, G., Tupper, A., Volentik, A., Waythomas, C.F. (2009). A multidisciplinary effort to assign realistic source parameters to models of volcanic ash-cloud transport and dispersion during eruptions. *J. Volcanol. Geotherm. Res.*, 186. doi: 10.1016/j.jvolgeores.2009.01.008.
- 30 National Centers for Environmental Prediction/National Weather Service/NOAA/U.S. Department of Commerce (2000), NCEP FNL Operational Model Global Tropospheric Analyses, continuing from July 1999, Research Data Archive at the National Center for Atmospheric Research, Computational and Information Systems Laboratory, Boulder, Colo. (Updated daily.), <https://doi.org/10.5065/D6M043C6>. Accessed 19 Dec 2017
- 35 Nelson, D., Yang, C., Kahn, R., Diner, D., & Mazzoni, D. (2008, Mar). Example Applications of the MISR Interactive EXplorer (MINX) Software Tool to Wildfire Smoke Plume Analyses. *Proc. SPIE*. doi: 10.1117/12.795087
- 40 Nelson, D., Garay, M., Kahn, R., & Dunst, B. (2013, Sep 17). Stereoscopic Height and Wind Retrievals for Aerosol Plumes with the MISR Interactive eXplorer (MINX). *Remote Sens.*, 5. doi: 10.3390/rs5094593



- 5 Rolph, G.D., Draxler, R.R., Stein, A.F., Taylor, A., Ruminski, M.G., Kondragunta, S., Zeng, J., Huang, H., Manikin, G., McQueen, J.T., & Davidson, J.T., 2009. Description and Verification of the NOAA Smoke Forecasting System: The 2007 Fire Season. *Wea. Forecasting*, 24, 361–378, doi: 10.1175/2008WAF2222165.1
- 10 Stein, A. F., G. D. Rolph, R. R. Draxler, B. Stunder and M. Ruminski (2009). "Verification of the NOAA Smoke Forecasting System: Model Sensitivity to the Injection Height." *Weather and Forecasting* 24(2): 379-394.
- 15 Stein, A., Draxler, R., Rolph, G., Stunder, J., and Cohen, M. (2016, Jan 14). NOAA's HYSPLIT Atmospheric Transport and Dispersion Modeling System. *Am. Meteorol. Soc.* doi: 10.1175/BAMS-D-14-00110.1
- 20 Stunder, B. J. B., J. L. Heffter and R. R. Draxler (2007). "Airborne volcanic ash forecast area reliability." *Weather and Forecasting* 22(5): 1132-1139.
- 25 Petrenko, M., Kahn, R., Chin, M., Soja, A., Kucsera, T., & Harshvardhan (2012, Sep 26). The use of satellite-measured aerosol optical depth to constrain biomass burning emissions source strength in the global model GOCART. *J. Geophys. Res.*, 117. doi: 10.1029/2012JD017870
- 30 Val Martin, M., Kahn, R., Logan, J., Paugam, R., Wooster, M., & Ichoku, C. (2012, Nov 28). Space-based observational constraints for 1-D fire smoke plume-rise models. *J. Geophys. Res.* doi: 10.1029/2012JD018370
- 35 Walter, C., S. R. Freitas, C. Kottmeier, I. Kraut, D. Rieger, H. Vogel and B. Vogel (2016). "The importance of plume rise on the concentrations and atmospheric impacts of biomass burning aerosol." *Atmospheric Chemistry and Physics* 16(14): 9201-9219.
- 40 NCEP GDAS website, <https://www.ncdc.noaa.gov/data-access/model-data/model-datasets/global-data-assimilation-system-gdas>, accessed January 2018:
- NASA Worldview website, <https://worldview.earthdata.nasa.gov>, accessed January 2018
- 35 NASA LADSWEB website, <https://ladsweb.modaps.eosdis.nasa.gov>, accessed December 2017
- NASA MISR Order and Customization Tool, <https://10dup05.larc.nasa.gov/MISR/cgi-bin/MISR>, accessed December 2017
- 40 University of Wyoming soundings archive, <http://weather.uwyo.edu/upperair/sounding.html>, accessed January 2018



Case Specific MISR Data, HYSPLIT run scripts, and BlueSky EMITIMES files, and VAAC/GVP advisories available upon request.

5

10

15

20 **Figure 1.** MINX Height Retrievals, measured from the geoid, for the Eyjafjallajokull volcano  
eruption plume, May 7, 2010. (a) Elevation map for the main plume. Each box represents a 0.55 km  
area where the height is displayed with darker colors on the low end and warmer colors on the high  
end. (b) MINX Height Profile, as a function of distance from the source. Terrain elevation is  
indicated by the green line. The injection height is ~ 5.8 km directly above the source, and remains  
25 at similar elevation downwind. (c) MINX Height Histogram, provides distribution of height  
retrievals without a wind correction, with the wind correction, and the cross/along track wind  
speeds.

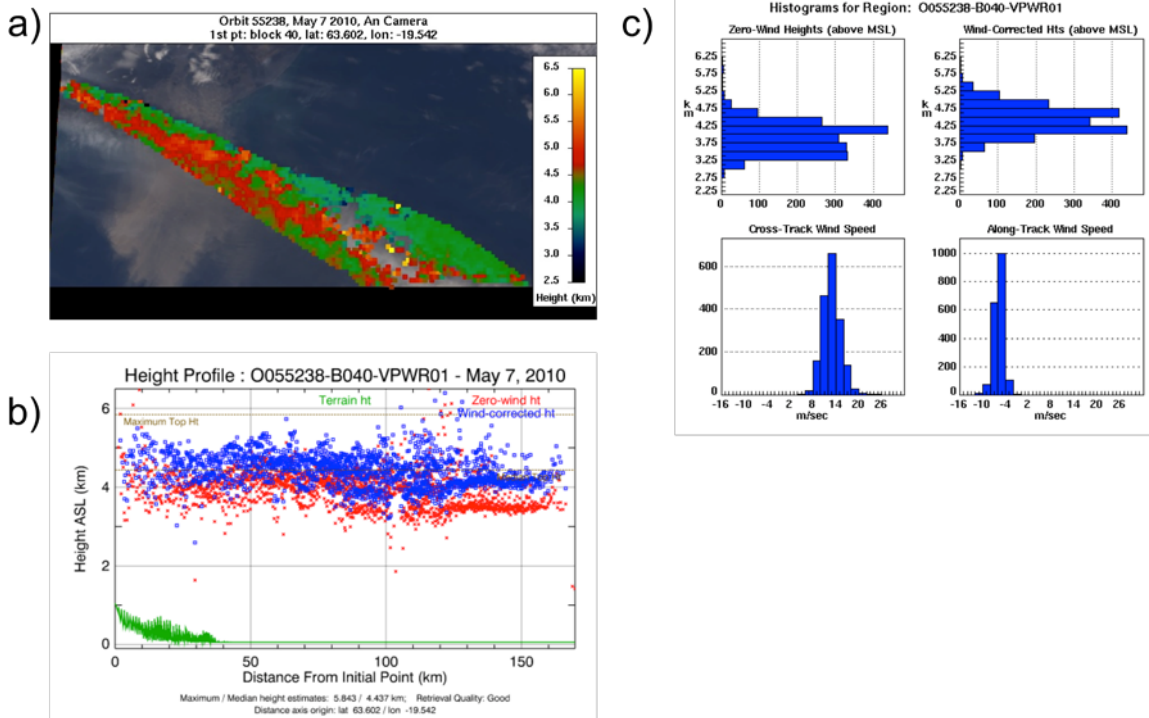


Table 1.

5

	Simulation Start Time	MISR Overpass Time	MINX Starting Location (° Latitude, ° Longitude) <sup>1</sup>	MINX Injection Height Mean Sea Level (km) <sup>2</sup>	Nominal Injection Height (MSL) at Time of MISR Overpass (km) <sup>3</sup>	PBL Height (MSL) at Time of MISR Overpass (km) <sup>4</sup>	BlueSky Heat Flux at Source (W/m <sup>2</sup> )	Particle Size (µm) and Mass Fraction (in Parenthesis)	Time of Snapshot
<u>Fort McMurray</u>	00:00 UTC May 6, 2016	18:35 UTC May 6, 2016	(56.779, -110.610)	4.2	3.5	2.9 (~3.0)	4.2 E+3	0.8 (1.0)	17:40 UTC May 7, 2017
<u>Fraser Plateau</u>	00:00 UTC Aug 3, 2017	19:35 UTC Aug 3, 2017	(53.039, -124.478)	4.2	3.6	3.5 (~3.1)	4.1 E+3	0.8 (1.0)	18:40 UTC Aug 4, 2017
<u>Thomas</u>	00:00 UTC Dec 10, 2017	18:45 UTC Dec 10, 2017	(34.450, -119.504)	5.5	1.9	1.6 (~3.3)	1.3 E+3	0.8 (1.0)	19:15 UTC Dec 13, 2017
<u>Eyjafjallajökull</u>	00:00 UTC May 7, 2010	12:35 UTC May 7, 2010	(56.779, -110.610)	5.8	6.7	~1.5	N/A	0.2 (.001), 0.6 (.005), 2.0 (.05), 6.0 (.2), 20 (.7), 60 (.044)	12:25 UTC May 9, 2010
<u>Etna</u>	00:00 UTC Jul 22, 2001	09:55 UTC Jul 22, 2001	(37.751, 14.993)	5.5	5.2	~1.2	N/A	0.2 (.001), 0.6 (.005), 2.0 (.05), 6.0 (.2), 20 (.7), 60 (.044)	09:55 UTC Jul 22, 2001
<u>Chikurachki</u>	12:00 UTC Apr 21, 2003 <sup>5</sup>	00:45 UTC Apr 22, 2003	(50.318, 155.457)	4.2	6.1	~1.3	N/A	0.6 (.008), 2.0 (.068), 6.0 (.254), 20 (.67)	01:15 UTC Apr 25, 2003





- 1) Wildfire cases have multiple source locations, but are shown as one representative location here
  - 2) Wildfire source locations also have their own injection heights determined by MINX. The highest injection height is identified on this table. Vertical resolution for the MINX injection height is around 275 m. The height listed here is the highest plume height recorded for each source.
  - 5 3) The nominal plume-rise height is given *at the time of MISR overpass*, for direct comparison with the MINX injection height. Figure 3 shows nominal plume rise and up-to-date meteorology *at the time that the snapshot was taken* for each case.
  - 4) All PBL heights marked with ~ are approximated from the nearest sounding location. Heights without parentheses or ~ were derived from the meteorological data at the time and location of the
  - 10 MISR overpass. The heights in parenthesis are above ground level and not above the geoid.
  - 5) The Chikurachki eruption simulation was started the day before the MISR overpass, because the overpass occurred close to the usual 00 UTC initialization. All other simulations had approximately 10 or more hours between initialization and the first snapshot.
- 15 **Figure 2.** Fort McMurray wildfire smoke plume evolution. (a) Day 2 sampling of the HYSPLIT 96-hour simulations that began on 06 May 2016, for 0 – 10 km, vertically integrated, qualitative smoke plume concentration based on MISR-MINX height initialization. Black outline indicates edges of visible smoke from satellite imagery and black star indicates source location (b) Same as (a), but using the nominal HYSPLIT height initialization. (c) MISR-Nominal initialization, qualitative smoke plume vertically integrated concentration differences. (d) MODIS true-color
- 20 image acquired on 07 May 2016. Red outline matches black outline from panels (a), (b), and (c) but is red for visibility.



2) Fort McMurray Wildfire Simulation - May 7, 2016 (17:40 UTC)

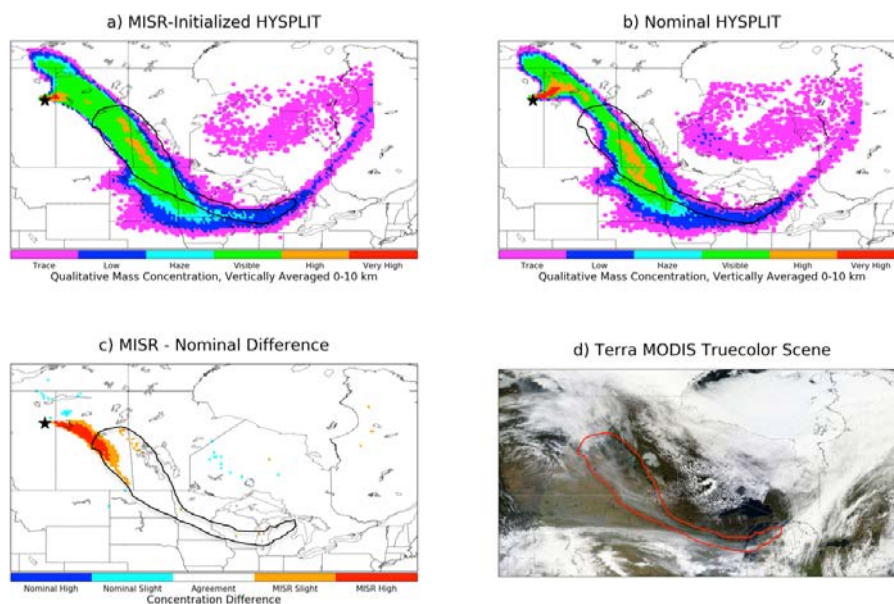


**Figure 3.** Atmospheric soundings at each of the nearest airports at the closest time to the snapshot for each case. The vertical axis is atmospheric pressure in mb on a log scale and the horizontal axis is temperature in °C. Horizontal lines indicate approximate elevation in m, isotherms are indicated as light grey lines from lower left to upper right, and those generally trending toward the upper left are dry adiabats. The rightmost dark black line shows the temperature sounding, and the one to the left represents the dewpoint profile. Wind speeds and directions are indicated by the barbs on the right side of each plot. The red line marks the planetary boundary layer, the blue line marks the injection height of the MISR-initialized simulation, and the green line marks the injection height of the nominal simulation at the hour of the snapshot. a) Fort McMurray, 08 May 2016 at 00Z: pbl ~ 2.5 km, MISR-initialized = 4.2 km, nominal ~ 2.4 km. b) Fraser Plateau, 05 August 2017 at 00Z: pbl ~ 3.1 km, MISR-initialized = 4.2 km, nominal ~ 2.7 km. c) Thomas Fire, 14 December 2017 at 00Z: pbl ~ 3.1 km, MISR-initialized = 5.5 km, nominal ~ 1.9 km. d) Eyjafjallajokull, 09 May 2010 at 12Z: pbl ~ 1.2 km, MISR-initialized = 5.8 km, nominal = 6.7 km. e) Etna, 23 July 2001 at 06Z: pbl ~ 1 km, MISR-initialized = 5.5 km, nominal = 5.2 km. f) Chikurachki, 25 April 2003 at 00Z: pbl ~ 1.3 km, MISR-initialized = 4.2 km, nominal = 6.1 km

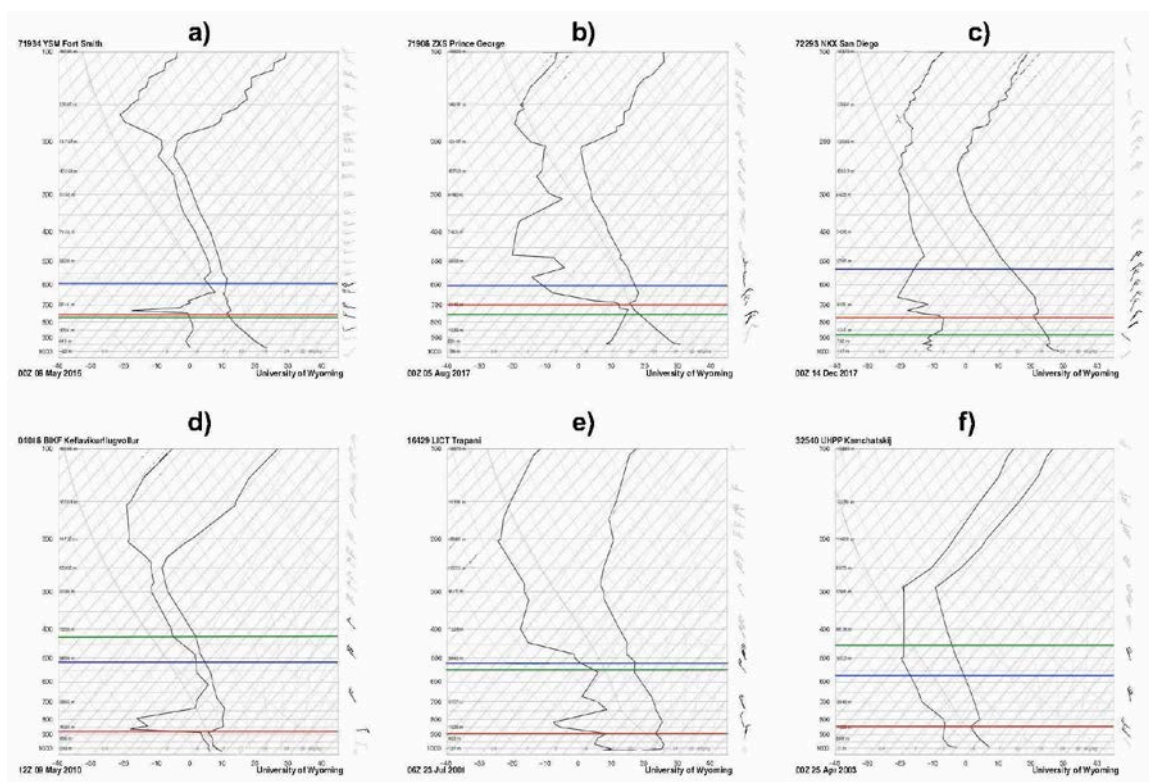


**Figure 4.** Same as Figure 2, but for the Fraser Plateau Fire plume on 04 August 2017. (a-b) Day 2 samplings of HYSPLIT 96-hour simulations that began on 03 August 2017, and (c) Day 2 difference plot. (d) MODIS true-color image acquired on 04 August 2017.



4) Fraser Plateau Wildfire Simulation - August 4, 2017 (18:40 UTC)

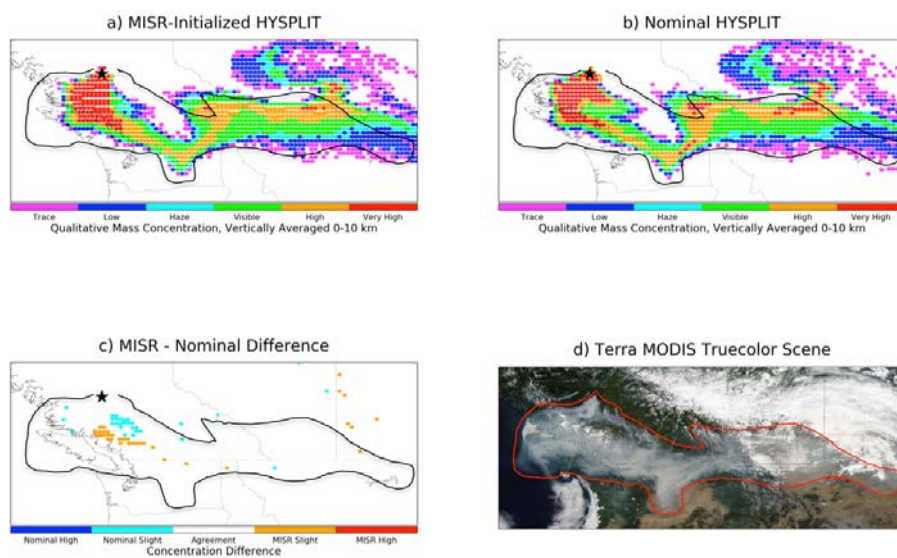
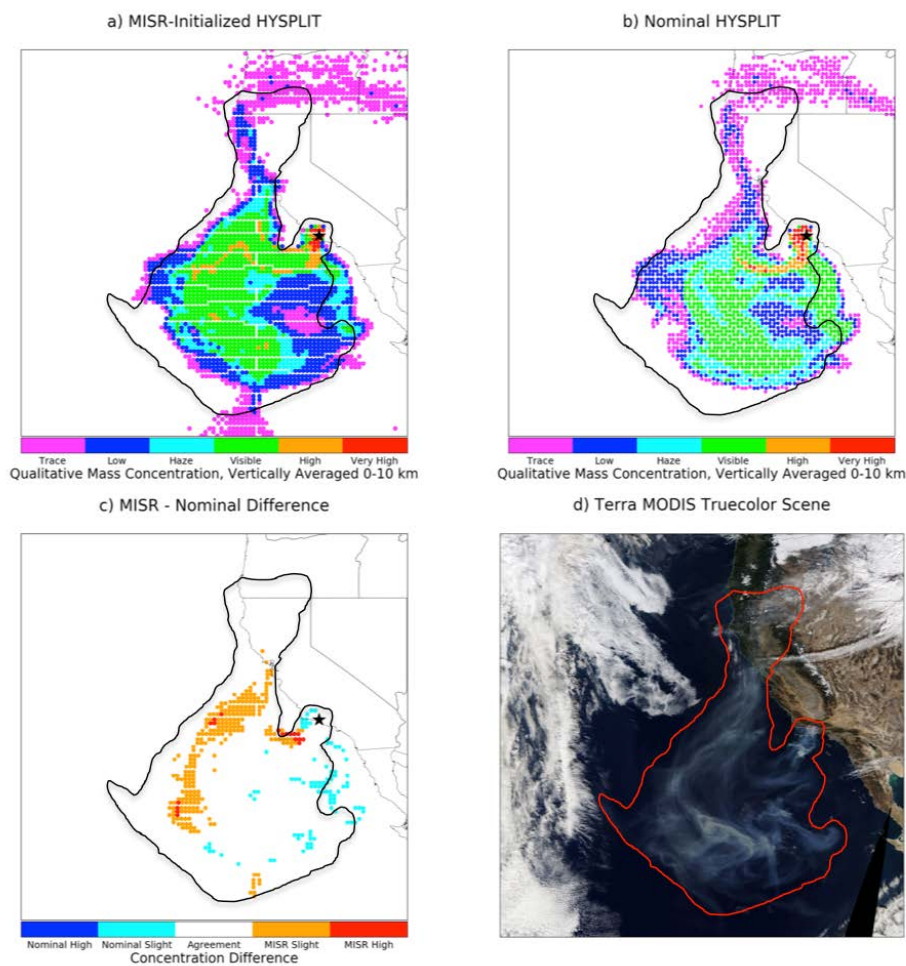


**Figure 5.** Same as Figure 2, but for the Thomas Fire plume, on 13 December 2017. (a-b) Day 4 samplings of HYSPLIT 96-hour simulations run with the GDAS 0.5° meteorology, beginning on 10 December 2017, and (c) Day 4 difference plot. (d) MODIS true-color image acquired on 13 December 2017.



5) Thomas Wildfire Simulation - December 13, 2017 (19:15 UTC)



5 **Figure 6.** Same as Figure 2, but for the Thomas Fire plume, on 13 December 2017 using NAM12 km meteorological data. (a-b) Day 4 samplings of HYSPLIT 96-hour simulations run with the NAM12 meteorology, beginning on 10 December 2017, and (c) Day 4 difference plot. (d) MODIS true-color image acquired on 13 December 2017.



6) Thomas Wildfire Simulation (With NAM12) - December 13, 2017 (19:15 UTC)

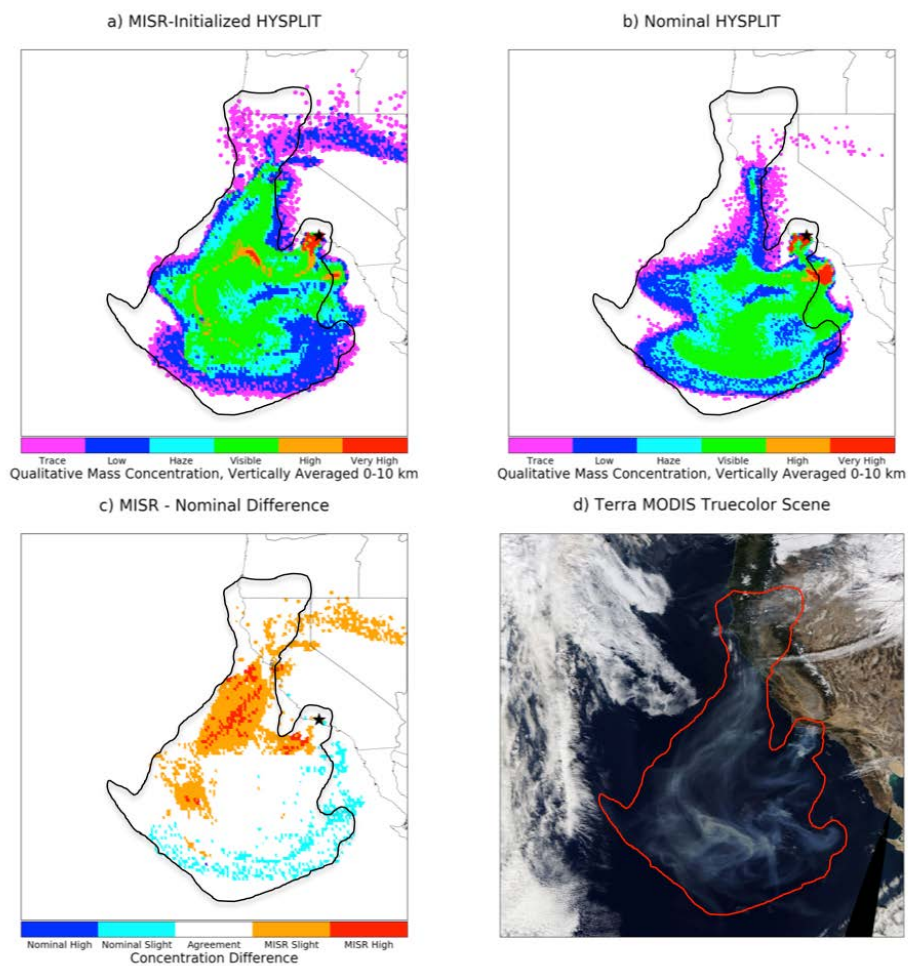


**Figure 7.** Same as Figure 2, but for the Eyjafjallajökull volcanic eruption plume, on 09 May 2010. (a-b) Day 3 samplings of HYSPLIT 96-hour simulations that began on 07 May 2010, and (c) Day 3 difference plot. (d) MODIS true-color image acquired on 09 May 2010.



7) Eyjafjallajökull Eruption Simulation - May 9, 2010 (12:25 UTC)

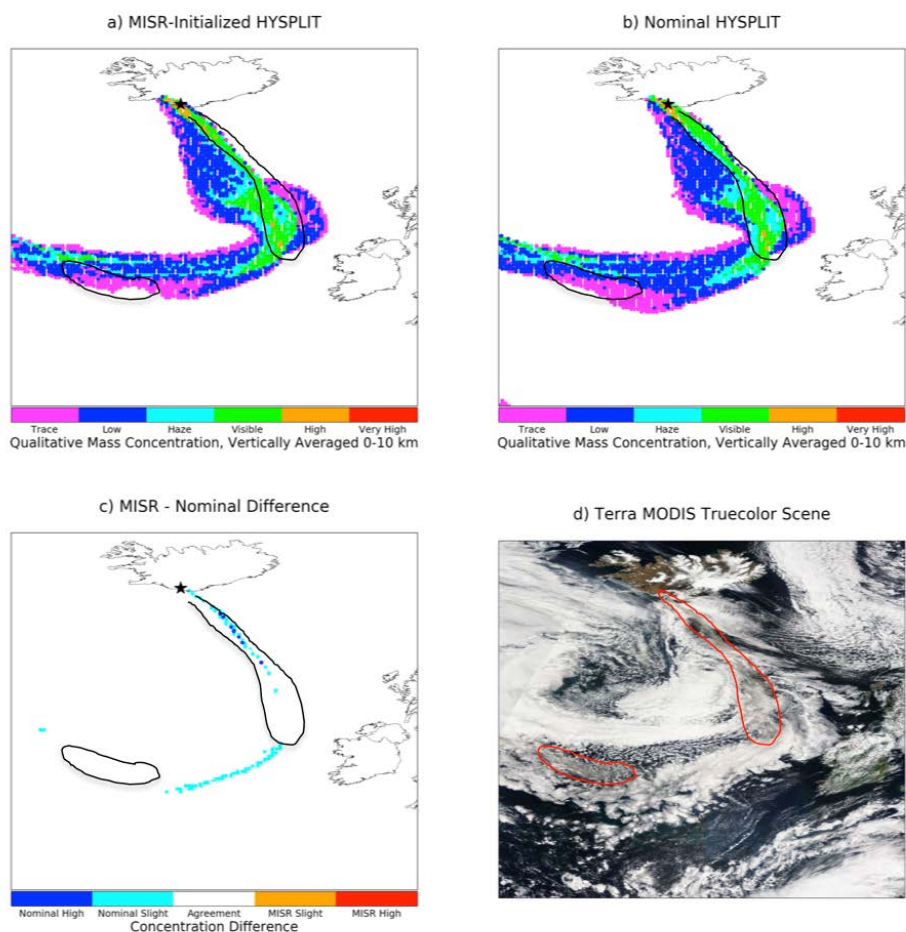


**Figure 8.** Same as Figure 2, but for the Mount Etna volcanic eruption plume, on 22 July 2001. (a-b) Day 1 samplings of HYSPLIT 96-hour simulations that began on 22 July 2001, (c) and Day 1 difference plot. (d) MODIS true-color image acquired on 22 July 2001.



8) Mount Etna Eruption Simulation - July 22, 2001 (09:55 UTC)

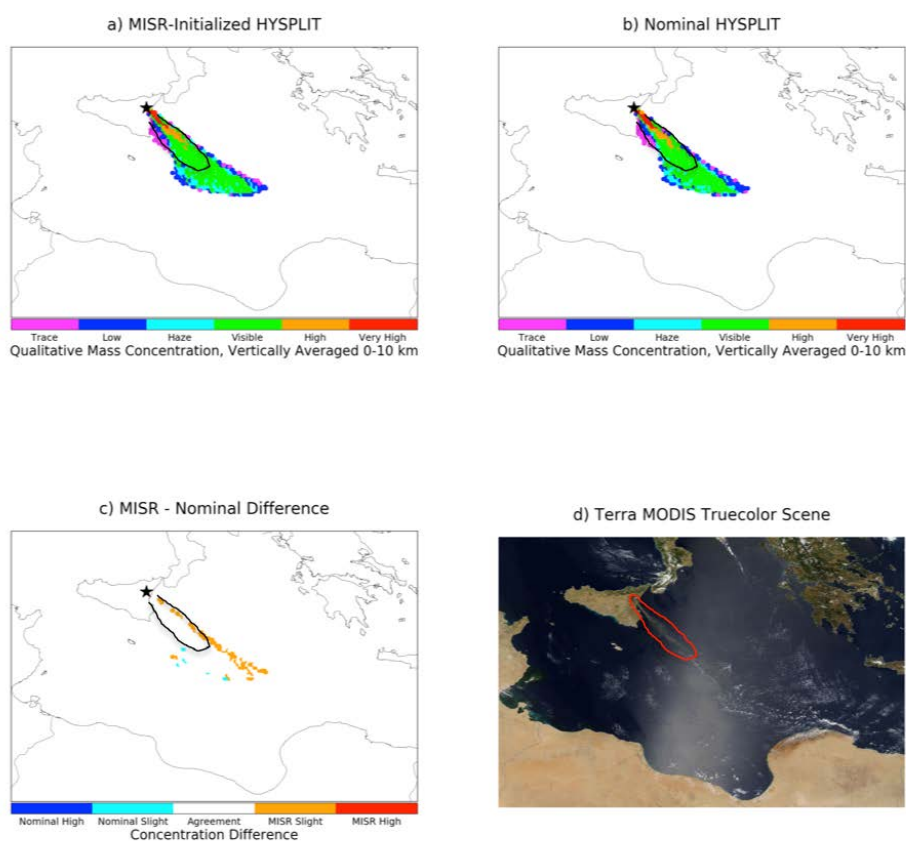


**Figure 9.** Same as Figure 2, but for the Chikurachki volcanic eruption plume, on 25 April 2003. (a-  
b) Day 4 samplings of HYSPLIT 96-hour simulations that began on 21 April 2003, and (c) Day 4  
5 difference plot. (d) MODIS true-color image acquired on 25 April 2003.





9) Chikurachki Eruption Simulation - April 25, 2003 (01:15 UTC)

